It follows that

$$C_S = (\lambda_1 - 4\gamma - \lambda_T)/4(\lambda_1 - \lambda_2),$$
$$D_S = (-\lambda_2 + 4\gamma + \lambda_T)/4(\lambda_1 - \lambda_2).$$

Table I gives the expected lifetimes for two-quantum annihilation and their relative intensity I_1/I_2 for various possible choices of the conversion rate γ, assuming that the triplet three-quantum annihilation rate is $\lambda_T = 7.14 \times 10^6$/sec as given by Ore and Powell[5] and that the singlet two-quantum rate is $\lambda_S = 8\times 10^9$/sec.[4] As noted in the text, the assumption of rapid conversion would require that these rates be increased by factors of about 2 or 3. For rapid conversion one then obtains $1/\lambda_2 \approx 2\times 10^{-10}$ sec in agreement with the experimental lifetime τ_1.

The dependence of the total rates for two- and three-quantum annihilation on the triplet-singlet conversion rate can be calculated in a similar manner. In the differential equations one replaces the probabilities P_S and P_T by the populations N_S and N_T, respectively, introduces constant rates of formation ($\frac{1}{4}$ for the singlet state and $\frac{3}{4}$ for the triplet state), and finally equates the derivatives to zero. This gives for the total rates:

$$\lambda_S N_S = \lambda_S(4\gamma + \lambda_T)/4\beta^2 \quad \text{(two-quantum)},$$
$$\lambda_T N_T = 3\lambda_T(4\gamma + \lambda_S)/4\beta^2 \quad \text{(three-quantum)}.$$

For λ_T small compared to γ and λ_S, one finds

$$\lambda_S N_S \approx 1 - 3\lambda_T/4\lambda_2,$$
$$\lambda_T N_T \approx 3\lambda_T/4\lambda_2.$$

For very rapid conversion, $\lambda_2 \to \lambda_S/4$, and hence

$$\lambda_T N_T \to 3\lambda_T/\lambda_S.$$

PHYSICAL REVIEW VOLUME 97, NUMBER 3 FEBRUARY 1, 1955

Matrix Elements in Superallowed Transitions*

MARK BOLSTERLI† AND EUGENE FEENBERG
Wayman Crow Laboratory, Washington University, St. Louis, Missouri
(Received July 23, 1954)

The nuclear matrix element for superallowed transitions between two states of an isobaric spin multiplet can be expressed in terms of a diagonal matrix element of the spin operator difference $\mathbf{S}_n - \mathbf{S}_p$. Known theoretical results on the nuclear matrix element in image transitions are summarized and the methods which have proved useful in the study of image transitions are extended to superallowed transitions within the lowest $T=1$ isobaric spin multiplet in the $4n$ series.

Experimental results indicate the actual occurrence of such transitions in Na^{20}, Al^{24}, P^{28}, Cl^{32} and Sc^{40}.

1. INTRODUCTION

THE known superallowed transitions now include the following types:

$$\begin{array}{lllll} a: & \Delta I=0, & T_i=T_f=\frac{1}{2} & (A=4n\pm 1), & \\ b: & \Delta I=\pm 1, & T_i=T_f=\frac{1}{2} & (A=7), & \\ c: & \Delta I_i=\pm 1, & \Delta T=\mp 1 & (A=4n+2), & (1) \\ d: & I_i=I_f=0, & T_i=T_f=1 & (A=4n+2), & \\ e: & \Delta I=0, & T_i=T_f=1 & (A=4n). & \end{array}$$

Types a to d are well known, but only recently has experimental work on short-lived radioactivities in the $4n$ nuclear series[1–5] indicated the actual occurrence of type e.[6] The list a to e does not exhaust the possible types of superallowed transitions. To see that others may occur, consider the approximation of spin- and charge-independent forces. In the $4n$ series the lowest supermultiplet containing a $T=1$ isobaric spin multiplet has the basic structure shown in Table I. Thus there are seven different final states coupled to the initial $(T_3=-1)$ state by nonvanishing Gamow-Teller matrix elements.

Now, by introducing a spin-dependent force, the seven distinct final states are spread out into a spectrum as illustrated in Fig. 1. The Fermi matrix element vanishes in all but the e-type transition. Other transitions with $\Delta T=0$ may occur, but they involve smaller decay energies and smaller decay matrix elements; hence they may be neglected in a preliminary discussion. The remaining three final states (those with $T=0$

TABLE I.

T	S	$I(L\neq 0)$
1	1	$L-1, L, L+1$
1	0	L
0	1	$L-1, L, L+1$

* Supported in part by the Office of Naval Research and the U. S. Atomic Energy Commission.
† Shell fellow 1952–1954; now National Science Foundation pre-doctoral fellow.
[1] N. W. Glass and J. R. Richardson, Phys. Rev. **93**, 942 (1954).
[2] Glass, Jensen, and Richardson, Phys. Rev. **90**, 320 (1953).
[3] Brackon, Henrikson, Martin, and Foster, Can. J. Phys. **32**, 223 (1954).
[4] A. C. Birge, Phys. Rev. **85**, 753 (1952).
[5] L. W. Alverez, Phys. Rev. **80**, 519 (1950).
[6] M. Bolsterli and E. Feenberg, Phys. Rev. **95**, 612 (1954).

derived from the lowest $[4^{n-1}31]$ supermultiplet) are not easily fixed on the energy scale. If one or more of these levels falls below the final state involved in the type e transition, a complicated decay scheme may occur with two or more strong superallowed components in the beta decay of the $T_3=-1$ isobar.

In this paper we begin with a summary of known theoretical results on the Gamow-Teller and Fermi matrix elements in image transitions (type a). The methods which have proved useful in the study of type a are then extended to type e. Finally the experimental evidence requiring the existence of type e transitions is exhibited and compared with theory.

2. GENERAL RELATIONS

The relation

$$ft|M|^2=\text{Constant} \tag{2}$$

and the definitions

$$|M|^2=r\left|\int 1\right|^2+\left|\int \boldsymbol{\sigma}\right|^2,$$

$$\begin{aligned} \left|\int 1\right|^2&=\sum_{m_f}|(f|\sum Q_k \text{ or } \sum Q_k^*|i)|^2,\\ \left|\int \boldsymbol{\sigma}\right|^2&=\sum_{m_f}|(f|\sum Q_k\boldsymbol{\sigma}_k \text{ or } \sum Q_k^*\boldsymbol{\sigma}_k|i)|^2,\\ Q&=\tfrac{1}{2}(\tau_1-i\tau_2),\\ Q^*&=\tfrac{1}{2}(\tau_1+i\tau_2), \end{aligned} \tag{3}$$

give the basic connection between theory and experiment in the analysis of superallowed transitions.

The most recent analysis[7] of image transitions (type a) places r on the range 0.75–1.15 in general agreement with earlier studies[8–11] and consistent with the weakly motivated but widespread preference for $r=1$. The theoretical estimates of $|\int\boldsymbol{\sigma}|^2$ are most secure at $A=1$, 3, 13, 15, 17, and 39; the analysis of image transitions in this group favors $r<1$ as does also recent accurate data[12] on the $0\rightarrow0$ transition at $A=14$. Fairly good all round agreement obtains for $r\sim0.8$. The values $r=0.8$ and

$$ft|M|^2\sim4700 \tag{4}$$

will be used in analyzing the data on fast transitions in the $4n$ series.

The Fermi matrix element occurring in transitions of

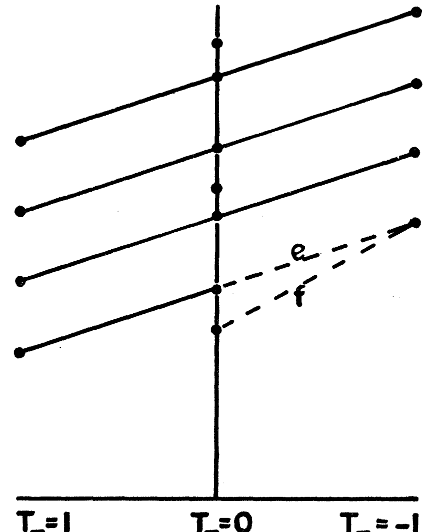

FIG. 1. A possible structure of the first LS supermultiplet containing $T=1$ multiplets. e denotes the superallowed β transition considered in this paper. f is another possible mode of decay.

types a, d, and e is given by the formula

$$\left|\int 1\right|^2=2T. \tag{5}$$

Deviations from this formula exceeding a few percent are not expected in the mass range covered by known superallowed transitions.[13]

A general formula for Gamow-Teller matrix elements in transitions of types a, b, and e can be derived from the commutation relations[14]

$$\begin{aligned} [T_1\pm iT_2,\, Y_{1u}\mp iY_{2u}]&=\pm 2Y_{3u},\\ [T_3,\, Y_{1u}\mp iY_{2u}]&=\mp(Y_{1u}\mp iY_{2u}), \end{aligned} \tag{6}$$

in which

$$\begin{aligned} T_i&=\tfrac{1}{2}\sum_1^A \tau_i^{(k)},\\ Y_{iu}&=\tfrac{1}{2}\sum_1^A \tau_i^{(k)}\sigma_u^{(k)},\quad u=x,y,z. \end{aligned} \tag{7}$$

If β, T, T_3 and β', T, T_3' represent the initial and final state quantum numbers, Eqs. (6) and (7) yield

$$\begin{aligned} (\beta',T,\mp(T-1)|Y_{1u}\pm iY_{2u}|\beta,T,\mp T)&\\ =\mp\left(\frac{2}{T}\right)^{\frac{1}{2}}&(\beta',T,\mp T|Y_{3u}|\beta,T,\mp T)\\ =\mp\left(\frac{2}{T}\right)^{\frac{1}{2}}&(\beta',T,\mp T|S_{nu}-S_{pu}|\beta,T,\mp T). \end{aligned} \tag{8}$$

[7] E. Feenberg, *The Shell Structure of the Nucleus* (Princeton University Press, Princeton, 1954).
[8] G. L. Trigg, Phys. Rev. **86**, 506 (1952).
[9] O. Kofoed-Hansen and A. Winther, Phys. Rev. **86**, 428 (1952).
[10] Wu, Rustad, Perez-Mendez, and Lidofsky, Phys. Rev. **87**, 1140 (1952).
[11] R. Nataf and R. Bouchez, Compt. rend. **234**, 86 (1952); Phys. Rev. **87**, 155 (1952).
[12] J. B. Gerhart, Phys. Rev. **95**, 288 (1954), R. Sherr and J. B. Gerhart, Phys. Rev. **91**, 909 (1953); also J. R. Penning and F. H. Schmidt, Phys. Rev. **94**, 779 (1954).
[13] L. A. Radicati, Proc. Phys. Soc. (London) **A66**, 139 (1953).
[14] E. Feenberg and G. E. Pake, *Notes on the Quantum Theory of Angular Momentum* (Addison-Wesley Press, Inc., Cambridge, 1953).

We observe that T_3 changes by one unit in the beta transition matrix element on the left while on the right $T_3'=T_3=\mp T$ (the value of T_3 in the initial state). The operator $\mathbf{S}_n-\mathbf{S}_p$ is simply the difference between the intrinsic spin operators of the neutron and proton groups. Equation (8) gives

$$\left|\int\boldsymbol{\sigma}\right|^2=\frac{2}{T}\sum_{m'}|(I,m',T,\mp T|\mathbf{S}_n-\mathbf{S}_p|I,m,T,\mp T)|^2. \quad (9)$$

In the special case $I'=I$,

$$\left|\int\boldsymbol{\sigma}\right|^2=\frac{2}{T}\frac{|\langle\mathbf{S}_n\cdot\mathbf{I}\rangle-\langle\mathbf{S}_p\cdot\mathbf{I}\rangle|^2}{I(I+1)}. \quad (10)$$

Here $\langle\;\rangle$ denotes a diagonal matrix element of the enclosed operator.

If either $\langle\mathbf{S}_n\cdot\mathbf{I}\rangle$ or $\langle\mathbf{S}_p\cdot\mathbf{I}\rangle$ vanishes, Eq. (10) reduces to

$$\left|\int\boldsymbol{\sigma}\right|^2=\frac{2}{T}\frac{|\langle\mathbf{S}\cdot\mathbf{I}\rangle|^2}{I(I+1)}. \quad (11)$$

3. SUMMARY OF RESULTS ON THE GAMOW-TELLER MATRIX ELEMENT FOR TYPE *a* TRANSITIONS

(i) *LS* Coupling, $S=1/2$

Under the stated condition the ground-state wave functions possess the maximum degree of symmetry in the space coordinates of the nucleons consistent with the exclusion principle. All spins are paired off in the even group of particles; hence either $\langle\mathbf{S}_n\cdot\mathbf{I}\rangle$ or $\langle\mathbf{S}_p\cdot\mathbf{I}\rangle$ vanishes and Eq. (10) can be rewritten in the form

$$\begin{aligned}\left|\int\boldsymbol{\sigma}\right|^2&=4\frac{|\langle\mathbf{S}\cdot\mathbf{I}\rangle|^2}{I(I+1)}\\&=(I+1)/I,\quad I=L+\tfrac{1}{2}\\&=I/(I+1),\quad I=L-\tfrac{1}{2}.\end{aligned} \quad (12)$$

This result was first derived by Wigner.[15] Equation (12) is also valid in jj coupling for doubly magic ±1 configurations ($A=1$, 3, 11, 13, 15, 17, 27, 29, 31, 33, 39, and 41). All spins are paired off in the closed-shell core and only the spin of a single nucleon or hole is involved in the evaluation of $\langle\mathbf{S}\cdot\mathbf{I}\rangle$.

(ii) Linear Combination of *LS* Coupling States, $S=1/2$

The wave function has the form

$$\psi=\alpha\psi_{L=I-\frac{1}{2}}+(1-\alpha^2)^{\frac{1}{2}}\psi_{L=I+\frac{1}{2}}, \quad (13)$$

a linear combination of the two *LS* coupling components possible for given I and $S=\frac{1}{2}$. Now,

$$\langle\mathbf{S}\cdot\mathbf{I}\rangle=\tfrac{1}{2}\{\alpha^2(I+1)-(1-\alpha^2)I\}, \quad (14)$$

and

$$\left|\int\boldsymbol{\sigma}\right|^2=\frac{1}{I(I+1)}[\alpha^2(I+1)-(1-\alpha^2)I]^2. \quad (15)$$

Equation (15), first derived by Trigg,[8] has proved useful in correlating observed values of the Gamow-Teller matrix element with the observed magnetic moment of the daughter nuclide.

Davidson[16] obtains numerical values for α^2 by an interpolation procedure involving the relation of the observed moment μ to theoretical values of the moment derived from the Schmidt single-particle and the Margenau-Wigner uniform models. The corresponding estimates for $|\int\boldsymbol{\sigma}|^2$ generally agree better with experiment than the pure *LS* coupling values.[8] The improvement at $A=29$ and 31 is particularly striking.

(iii) Odd Group Model

A simple explicit formula expressing $|\int\boldsymbol{\sigma}|^2$ in terms of μ can be derived from the assumption that all the angular momentum and magnetic properties are carried by the odd group of particles (odd group model). The moment operator,

$$\begin{aligned}\boldsymbol{\mu}&=g_l\mathbf{L}+g_s\mathbf{S}\\&=g_l\mathbf{I}+(g_s-g_l)\mathbf{S},\end{aligned} \quad (16)$$

now yields

$$\mu=g_lI+(g_s-g_l)\langle\mathbf{S}\cdot\mathbf{I}\rangle/(I+1), \quad (17)$$

or

$$\langle\mathbf{S}\cdot\mathbf{I}\rangle=(I+1)(\mu-g_lI)/(g_s-g_l). \quad (18)$$

This relation is consistent with the doublet description of the nuclear state [Eq. (13)], but holds also for an arbitrary linear combination of multiplet components. From Eqs. (11) and (18) we obtain Winther's formula,[17]

$$\left|\int\boldsymbol{\sigma}\right|^2=4\frac{I+1}{I}\left(\frac{\mu-g_lI}{g_s-g_l}\right)^2. \quad (19)$$

Our derivation of Winther's semiempirical formula is at fault in combining a relation [Eqs. (10) and (11)] derived from the assumption that the isobaric spin T is a good quantum number with a consequence [Eq. (18)] of the odd group model (in which the isotopic spin is not, as a rule, a constant of motion). Consequently, in default of a more satisfactory derivation, Eq. (19) must still be interpreted as a more or less useful semiempirical interpolation formula.

(iv) Symmetrical Interpolation Formulas

A more rigorous analysis of image transitions becomes possible when the magnetic moments of both members of mirror pairs are known. This statement follows from the fact that the sum of the moments obeys simpler relations than either moment alone.[18]

[15] E. P. Wigner, Phys. Rev. **56**, 519 (1939).

[16] J. P. Davidson, Phys. Rev. **85**, 432 (1952).

[17] A. Winther, Physica **18**, 1079 (1952).

[18] R. G. Sachs, Phys. Rev. **69**, 611 (1946).

The nucleon moment operator,

$$\mathbf{\mu}=g_l^p \sum \mathbf{l}_k \tfrac{1}{2}(1-\tau_3^{(k)})+g_s^n \sum \mathbf{S}_k \tfrac{1}{2}(1+\tau_3^{(k)}) +g_s^p \sum \mathbf{S}_k \tfrac{1}{2}(1-\tau_3^{(k)}), \quad (20)$$

in the form

$$\mathbf{\mu}=\tfrac{1}{2}g_l^p\mathbf{I}+\tfrac{1}{2}(g_s^n+g_s^p-g_l^p)\mathbf{S} +\tfrac{1}{4}(g_s^n-g_s^p)\sum \tau_3^k\mathbf{\sigma}_k-\tfrac{1}{2}g_l^p \sum \tau_3^k\mathbf{l}_k, \quad (21)$$

gives immediately the result

$$\langle \mathbf{S}\cdot\mathbf{I}\rangle=(I+1)\frac{\mu(T_3=\frac{1}{2})+\mu(T_3=-\frac{1}{2})-I}{g_s^n+g_s^p-1}, \quad (22)$$

after setting $g_l^p=1$.

The introduction of Eq. (22) into Eq. (11) for $|\int\mathbf{\sigma}|^2$ is justified only if $\langle\mathbf{S}_n\cdot\mathbf{I}\rangle$ or $\langle\mathbf{S}_p\cdot\mathbf{I}\rangle$ vanishes, and this is physically plausible only under conditions which make the doublet description of Eq. (13) a good approximation. If one assumes the doublet description,[7]

$$\mu(\tfrac{1}{2})+\mu(-\tfrac{1}{2}) =I+(g_s^n+g_s^p-1)\frac{\alpha^2(I+1)-(1-\alpha^2)I}{2(I+1)}, \quad (23)$$

$$\left|\int\mathbf{\sigma}\right|^2=4\frac{I+1}{I}\left[\frac{\mu(\frac{1}{2})+\mu(-\frac{1}{2})-I}{g_s^n+g_s^p-1}\right]^2. \quad (24)$$

The sum $\mu(\frac{1}{2})+\mu(-\frac{1}{2})$ is expected to depend relatively little on the amount and form of exchange moment operators. When both left- and right-hand members of Eq. (24) are known experimentally deviations from equality of the two members may yield information on the magnitude of quartet components in the ground state wave functions and on relativistic corrections to the moment operators.[19,20]

(v) *jj* Coupling

The magnetic properties of n neutrons and protons in a j shell are described by the moment operator,

$$\mathbf{\mu}=g_j^n \sum \mathbf{j}_k(1+\tau_3^k)/2+g_j^p \sum \mathbf{j}_k(1-\tau_3^k)/2 \quad (25)$$

in which $g_j^n=\mu_j^n/j$ and $g_j^p=\mu_j^p/j$ are the Landé g factors for single nucleons in j orbitals. Equation (25) gives the moment formula:

$$\mu=\frac{1}{2}(\mu_j^n+\mu_j^p)\frac{I}{j}+(\mu_j^n-\mu_j^p)\frac{\langle(\mathbf{I}_n-\mathbf{I}_p)\cdot\mathbf{I}\rangle}{j(I+1)}$$
$$=\frac{1}{2}(\mu_j^n+\mu_j^p)\frac{I}{j} +(-1)^{j-l-\frac{1}{2}}\frac{l+\frac{1}{2}}{j}(\mu_j^n-\mu_j^p)\frac{\langle(\mathbf{S}_n-\mathbf{S}_p)\cdot\mathbf{I}\rangle}{I+1}. \quad (26)$$

[19] H. Primakoff, Phys. Rev. **72**, 118 (1947).
[20] G. Breit and R. M. Thaler, Phys. Rev. **89**, 1177 (1953).

Equations (10) and (26) together yield Mayer's formula,[21]

$$\left|\int\mathbf{\sigma}\right|^2=\frac{I+1}{I}\left(\frac{j}{l+\frac{1}{2}}\right)^2 \times\left(\frac{2\mu(T_3=\pm\frac{1}{2})-(\mu_j^n+\mu_j^p)I/j}{\mu_j^n-\mu_j^p}\right)^2. \quad (27)$$

Equation (26) also implies

$$\mu(T_3=\tfrac{1}{2})-\mu(T_3=-\tfrac{1}{2}) =(-1)^{j-l-\frac{1}{2}}\frac{2l+1}{j}(\mu_j^n-\mu_j^p)\frac{\langle(\mathbf{S}_n-\mathbf{S}_p)\cdot\mathbf{I}\rangle}{I+1}, \quad (28)$$

and yields the symmetrical interpolation formula,[7]

$$\left|\int\mathbf{\sigma}\right|^2=\frac{I+1}{I}\left(\frac{j}{l+\frac{1}{2}}\right)^2\left(\frac{\mu(\frac{1}{2})-\mu(-\frac{1}{2})}{\mu_j^n-\mu_j^p}\right)^2. \quad (29)$$

These relations are particularly useful when the jj coupling configuration provides two or more linearly independent wave functions with $T=\frac{1}{2}$ and the required value of I. In such cases neither $\mu(T_3)$ nor $|\int\mathbf{\sigma}|^2$ can be computed independently without information on the correct linear combination of component wave functions in the description of the ground state.

(vi) Special Case: $A=3$

The wave function

$$\psi=\alpha\phi(^2S_{\frac{1}{2}})+(1-\alpha^2)^{\frac{1}{2}}\phi(^4D_{\frac{1}{2}}) \quad (30)$$

with $\alpha^2=0.96$ has been derived from the assumption of strong two particle tensor interactions between pairs of nucleons.[22] In evaluating the D state contribution to the Gamow-Teller matrix element, $\mathbf{S}_n-\mathbf{S}_p$ may be replaced by $\frac{1}{3}\mathbf{S}$. Equation (11) yields[23]

$$\left|\int\mathbf{\sigma}\right|^2=[-\tfrac{3}{4}\alpha^2-\tfrac{1}{4}(1-\alpha^2)]^2\frac{4}{I(I+1)} =\tfrac{1}{3}(2\alpha^2+1)^2=2.88, \quad (31)$$

possibly a little low, but not certainly inconsistent with the experimental requirements. For comparison, Eq. (24), based on the absence of a quartet component, gives only 2.58.

4. TYPE e: $\Delta I=0$, $T_i=T_f=1$ ($A=4n$)

(i) Both Odd Groups of the Parent System Are in Doublet States ($S_n=S_p=1/2$)

Under these conditions the general wave function

$$\psi=a_0\psi_{L=I,\,S=0}+a_1\psi_{L=I-1,\,S=1} +a_2\psi_{L=I,\,S=1}+a_3\psi_{L=I+1,\,S=1} \quad (32)$$

[21] M. G. Mayer, Indiana Conference on Beta Spectroscopy and Nuclear Structure, 1953 (unpublished).
[22] R. L. Pease and H. Feshbach, Phys. Rev. **88**, 948 (1952).
[23] J. M. Blatt, Phys. Rev. **89**, 86 (1953).

may contain both singlet and triplet components and possibly three different values of L. Equations (9) and (32) give

$$\left|\int \boldsymbol{\sigma}\right|^2 = 8a_0^2a_2^2 \leqq 2. \tag{33}$$

(ii) I_n and I_p Are Good Quantum Numbers; $S_n = S_p = 1/2$

The equivalence relations,

$$\mathbf{S}_q \rightarrow \mathbf{I}_q \frac{\langle \mathbf{S}_q \cdot \mathbf{I}_q \rangle}{I_q(I_q+1)}, \quad q = n \text{ or } p, \tag{34}$$

make possible the reduction of Eq. (10) to

$$\begin{aligned}\left|\int \boldsymbol{\sigma}\right|^2 &= \frac{2}{I(I+1)}\left|\frac{\langle \mathbf{S}_n\cdot\mathbf{I}_n\rangle\langle \mathbf{I}_n\cdot\mathbf{I}\rangle}{I_n(I_n+1)} - \frac{\langle \mathbf{S}_p\cdot\mathbf{I}_p\rangle\langle \mathbf{I}_p\cdot\mathbf{I}\rangle}{I_p(I_p+1)}\right|^2 \\ &= \frac{1}{2I(I+1)}\left| I(I+1)\left\{\frac{\langle \mathbf{S}_n\cdot\mathbf{I}_n\rangle}{I_n(I_n+1)} - \frac{\langle \mathbf{S}_p\cdot\mathbf{I}_p\rangle}{I_p(I_p+1)}\right\} \right. \\ &\quad + (I_n - I_p)(I_n+I_p+1) \\ &\quad \left. \times \left\{\frac{\langle \mathbf{S}_n\cdot\mathbf{I}_n\rangle}{I_n(I_n+1)} + \frac{\langle \mathbf{S}_p\cdot\mathbf{I}_p\rangle}{I_p(I_p+1)}\right\}\right|^2. \end{aligned} \tag{35}$$

Equation (18) can be used to estimate $\langle \mathbf{S}_n\cdot\mathbf{I}_n\rangle$ and $\langle \mathbf{S}_p\cdot\mathbf{I}_p\rangle$ if the magnetic moments of suitable $4n\pm1$ nuclides are known. These nuclides must have the number of nucleons in the odd group equal to $\frac{1}{2}A-1$ in one and to $\frac{1}{2}A+1$ in the other.

(iii) *jj* Coupling; One Hole and One Particle

The ground states of ${}_{15}P_{13}$, ${}_{17}Cl_{15}$, ${}_{19}K_{17}$, and ${}_{21}Sc_{19}$ belong in this category. The preceding relations [Eqs. (34) and (35)] remain valid with the advantage that $\langle \mathbf{S}_n\cdot\mathbf{I}_n\rangle$ and $\langle \mathbf{S}_p\cdot\mathbf{I}_p\rangle$ can be evaluated explicitly. Thus,

$$\begin{aligned} 2\langle \mathbf{S}_n\cdot\mathbf{I}_n\rangle &= j_n+1, \quad j_n = l_n+\tfrac{1}{2} \\ &= -j_n, \quad j_n = l_n - \tfrac{1}{2}. \end{aligned} \tag{36}$$

Special Cases

For $j_n = l_n+\frac{1}{2}$, $j_p = l_p+\frac{1}{2}$,

$$\left|\int \boldsymbol{\sigma}\right|^2 = \frac{(j_n-j_p)^2}{8I(I+1)j_n^2 j_p^2} \times |I(I+1)-(j_n+j_p)(j_n+j_p+1)|^2. \tag{37}$$

For $j_n = l_n+\frac{1}{2}$, $j_p = l_p-\frac{1}{2}$,

$$\left|\int \boldsymbol{\sigma}\right|^2 = \frac{(j_n+j_p+1)^2}{8I(I+1)j_n^2(j_p+1)^2} \times |I(I+1)-(j_p-j_n)(j_p-j_n+1)|^2. \tag{38}$$

Interchange of j_n and j_p in Eq. (38) gives $|\int\boldsymbol{\sigma}|^2$ for $j_n = l_n-\frac{1}{2}$, $j_p = l_p+\frac{1}{2}$.

For $j_n = l_n-\frac{1}{2}$, $j_p = l_p-\frac{1}{2}$,

$$\left|\int \boldsymbol{\sigma}\right|^2 = \frac{(j_n-j_p)^2}{8I(I+1)(j_n+1)^2(j_p+1)^2} \times |I(I+1)-(j_n+j_p+1)(j_n+j_p+2)|^2. \tag{39}$$

(iv) *jj* Coupling: $j_n = j_p = j$, $l_n = l_p = l$

The ground states of ${}_{11}Na_9$ and ${}_{13}Al_{11}$ may be discussed under this heading. Equation (10) yields

$$\begin{aligned}\left|\int \boldsymbol{\sigma}\right|^2 &= \frac{2}{I(I+1)(2l+1)^2}|\langle \mathbf{I}_n\cdot\mathbf{I}\rangle - \langle \mathbf{I}_p\cdot\mathbf{I}\rangle|^2 \\ &= \frac{2}{I(I+1)(2l+1)^2}|\langle \mathbf{I}_n^2\rangle - \langle \mathbf{I}_p^2\rangle|^2. \end{aligned} \tag{40}$$

In ${}_{13}Al_{11}$, $I=4$, $l=2$, $\langle \mathbf{I}_p^2\rangle = 35/4$, $\langle \mathbf{I}_n^2\rangle \geqq 15/4$; hence

$$\left|\int \boldsymbol{\sigma}\right|^2 \leqq 1/10, \tag{41}$$

if we exclude the unlikely possibility that the accurate description of the odd-neutron group requires a large admixture of component states with $I_n = 7/2$ or $9/2$.

Interpolation formulas similar to Eqs. (27) and (29) can be derived immediately from Eqs. (10) and (26):

$$\left|\int \boldsymbol{\sigma}\right|^2 = \frac{I+1}{2I}\left(\frac{j}{l+\frac{1}{2}}\right)^2 \times \left(\frac{2\mu(T_3=\pm1) - (\mu_j^n+\mu_j^p)I/j}{\mu_j^n - \mu_j^p}\right)^2, \tag{42}$$

$$\left|\int \boldsymbol{\alpha}\right|^2 = \frac{I+1}{2I}\left(\frac{j}{l+\frac{1}{2}}\right)^2\left(\frac{\mu(1)-\mu(-1)}{\mu_j^n-\mu_j^p}\right)^2. \tag{43}$$

Introducing $I=4$, $j=5/2$, $l=2$, and $\mu({}_{11}Na_{13}) = 1.688$ into Eq. (42), we get

$$\left|\int \boldsymbol{\sigma}\right|^2 \sim 0.021 \tag{44}$$

for the type e superallowed component in the decay of ${}_{13}Al_{11}$.

5. EVIDENCE FOR SUPERALLOWED TRANSITIONS IN THE $4n$ SERIES

Recent experimental studies[1–5] indicate the existence of a group of superallowed transitions characterized by $T=1$, $\Delta I=0$, $A=4n$. The transitions probably occur as strong components in the decay of ${}_{13}Al_{11}$, ${}_{15}P_{13}$, ${}_{17}Cl_{15}$, and ${}_{21}Sc_{19}$. Also a weak superallowed component may produce observable effects in the decay of ${}_{11}Na_9$.

In principle ${}_7N_5$ and ${}_5B_3$ should also decay through superallowed channels, but the theoretical estimates of the branching ratios in these examples places the intensity of the superallowed component below the threshold for observation with present experimental techniques.

The information available for locating the lowest $T=T$, $T_3=0$ level (in the level diagram of the stable isobar) may be illustrated by the example at $A=24$. The disintegration energies of ${}_{11}Na_{13}$ and of ${}_{12}Mg_{11}$ are known. This information and the approximate relation

$$M(T=1,\ {}_{12}Mg_{12})-M(T=1,\ {}_{11}Na_{13}) \cong M(T=\tfrac{1}{2},\ {}_{12}Mg_{11})-M(T=\tfrac{1}{2},\ {}_{11}Na_{12}) \quad (45)$$

place the lowest $T=1$ state in ${}_{12}Mg_{12}$ at the excitation energy 9.52 Mev. This value lies above the limit of alpha stability (at 9.33 Mev) in agreement with the observation of delayed α's associated with the decay of ${}_{13}Al_{11}$. Information on γ transitions in ${}_{12}Mg_{12}$ may eventually give an independent check on the location of the $T=1$ level. The mass difference $M({}_{13}Al_{11})-M({}_{12}Mg_{12})$ can also be determined in several ways: (a) from an estimate of the Coulomb energy difference, (b) from the threshold in the pn reaction on ${}_{12}Mg_{12}$, and (c) from the energy of the most energetic positrons observed in the decay of ${}_{13}Al_{11}$ (for ${}_{13}Al_{11}$ this energy has not been reported, but values are given for ${}_{15}P_{13}$ and ${}_{17}Cl_{15}$).

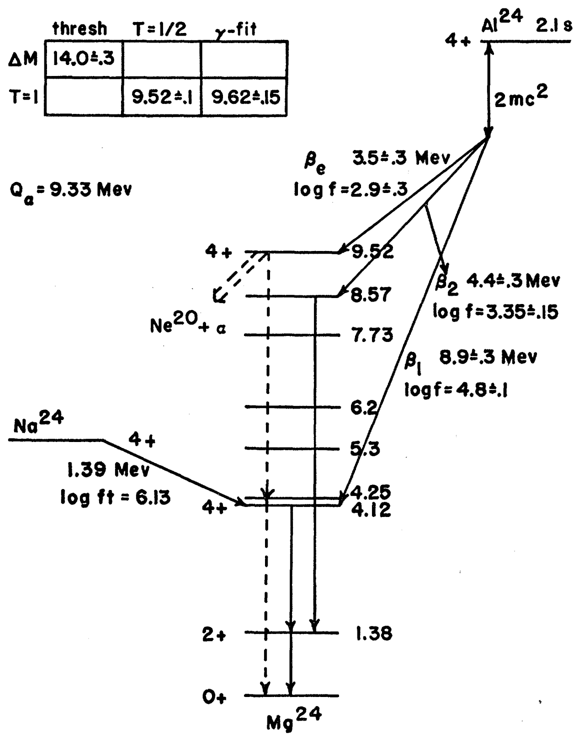

FIG. 2. Tentative decay scheme for Al[24]. The box in the upper left corner gives values for $\Delta M(Al^{24}-Mg^{24})$ and the height of the $T=1$ level, obtained by the methods which label the columns.

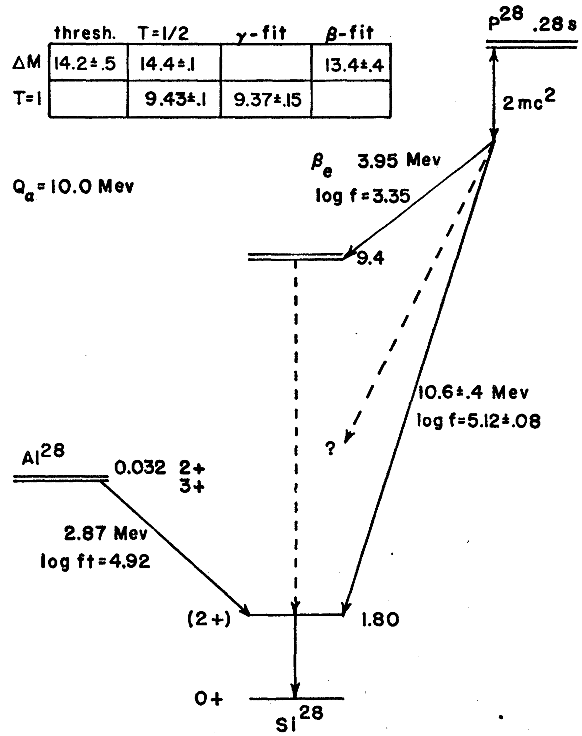

FIG. 3. Partial decay scheme for P[28].

${}_{13}Al_{11}$, Fig. 2

The diagram shown is supported by all the recent work on ${}_{11}Na_{13}$, ${}_{12}Mg_{12}$, ${}_{13}Al_{11}$, and ${}_{12}Mg_{11}$. The 4.25-Mev level is probably not fed by β's since it is not observed in the decay of Na^{24}. Turner's work[24] indicates that, except for the $T=1$ level, the only known levels associated with the decay are those at 8.57 Mev and at 4.12 Mev (the latter is reached by the Na^{24} β decay). The $T=1$ level at 9.52 Mev may account for the observation of α's in the decay of Al^{24} (the threshold for the emission of α's by Mg^{24} is 9.33 Mev). The assumption that β^+ and β^- transitions to the 4.12-Mev level have nearly equal transition matrix elements yields a partial half-life $t_{\frac{1}{2}}({}_{13}Al_{11}$, 4.12-Mev level$)=18$ to 30 sec, with a branching ratio of approximately 10 percent. If the transition to the 8.57-Mev level is allowed unfavored, it has a minimum partial half-life of about 10 sec and a maximum branching ratio of about 20 percent. If no other important transitions are assumed,

$$\begin{gathered} 70\text{ percent} \leqq BR(\beta_e) \leqq 90\text{ percent}, \\ 3\text{ sec} \geqq t_{\frac{1}{2}}(\beta_e) \geqq 2.34\text{ sec}, \\ 3.25\pm0.3 \leqq \log ft(\beta_e) \leqq 3.4\pm0.3. \end{gathered} \quad (46)$$

Equations (41) and (44) give $|M|^2 \sim 1.6-1.7$, close to the minimum possible value. Inserting this into the

[24] O. H. Turner, Australian J. Sci. Research 6, 380 (1953).

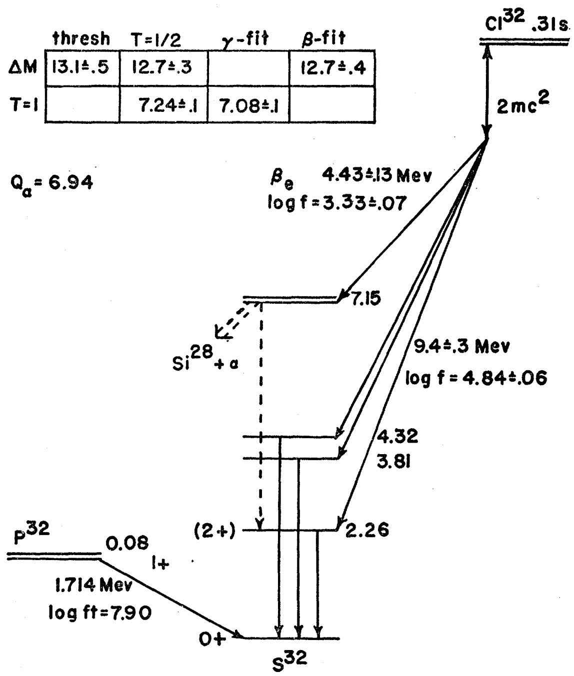

FIG. 4. A possible decay scheme for Cl^{32}.

preceding inequality, we get

$$3.5\pm0.3 \leqq \log ft|M|^2 \leqq 3.6\pm0.3, \quad (47)$$

consistent with $ft|M|^2 \sim 4700$, $\log ft|M|^2 = 3.67$.

${}_{15}P_{13}$, Fig. 3

In ${}_{15}P_{13}$, the decay scheme is probably complex. The ground state and the low-lying first excited state in ${}_{13}Al_{15}$ have spins 3+ and 2+, respectively.[25] The order of these two levels may be reversed in one or both of ${}_{14}Si_{14}$ and ${}_{15}P_{13}$; the transition considered here as the superallowed component is that between the ground state of ${}_{15}P_{13}$ and the corresponding state in ${}_{14}Si_{14}$.

Since the number of allowed β^+ components in the decay of ${}_{15}P_{13}$ is unknown, only a minimum estimate of the branching ratio into the type e component can be given. Since $|\int 1|^2 = 2$, we must have $\log ft(\beta_e) \leqq 3.45$; this gives $t_{\frac{1}{2}}(\beta_e) \leqq 1.3$ sec or $BR(\beta_e) \geqq 20$ percent.

[25] Sheline, Johnson, Bell, Davis, and McGowan, Phys. Rev. **94**, 1642 (1954).

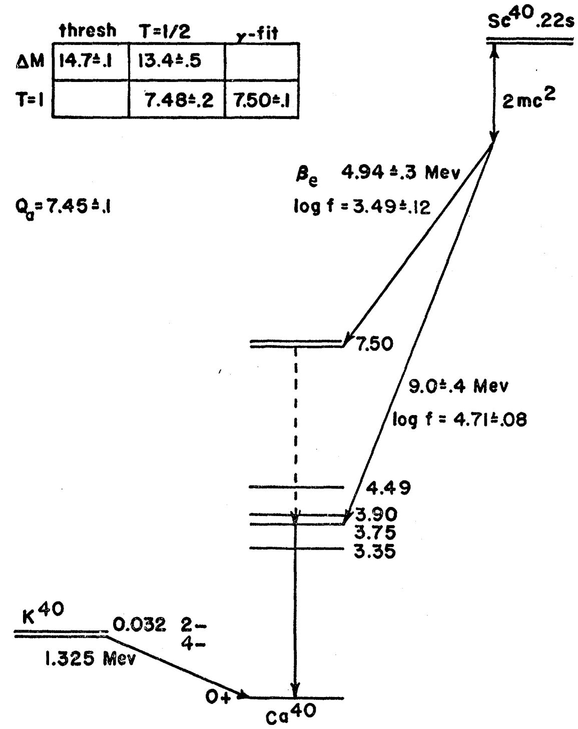

FIG. 5. Tentative decay scheme for Sc^{40}.

${}_{17}Cl_{15}$, Fig. 4

The close doublet structure exhibited by ${}_{15}P_{17}$ presumably occurs also in ${}_{17}Cl_{15}$ and the lowest $T=1$ states of ${}_{16}S_{16}$. The γ's observed in the decay of ${}_{17}Cl_{15}$ fit known levels of ${}_{16}S_{16}$ as shown. Delayed α's observed in the decay of ${}_{17}Cl_{15}$ may come from the lowest $T=1$ level of ${}_{16}S_{16}$ since the excitation energy (7.15 Mev) is greater than Q_α (6.94 Mev).

A procedure like that used for ${}_{15}P_{13}$ gives $BR(\beta_e) \geqq 25$ percent.

${}_{21}Sc_{19}$, Fig. 5

A tentative decay scheme is shown. Here a branching ratio ≥ 25 percent is required for the type e component. No delayed α's have been observed in the decay of Sc^{40}, consistent with the assumption that there is no branching to states higher than the first $T=1$ level.